Figure 1.

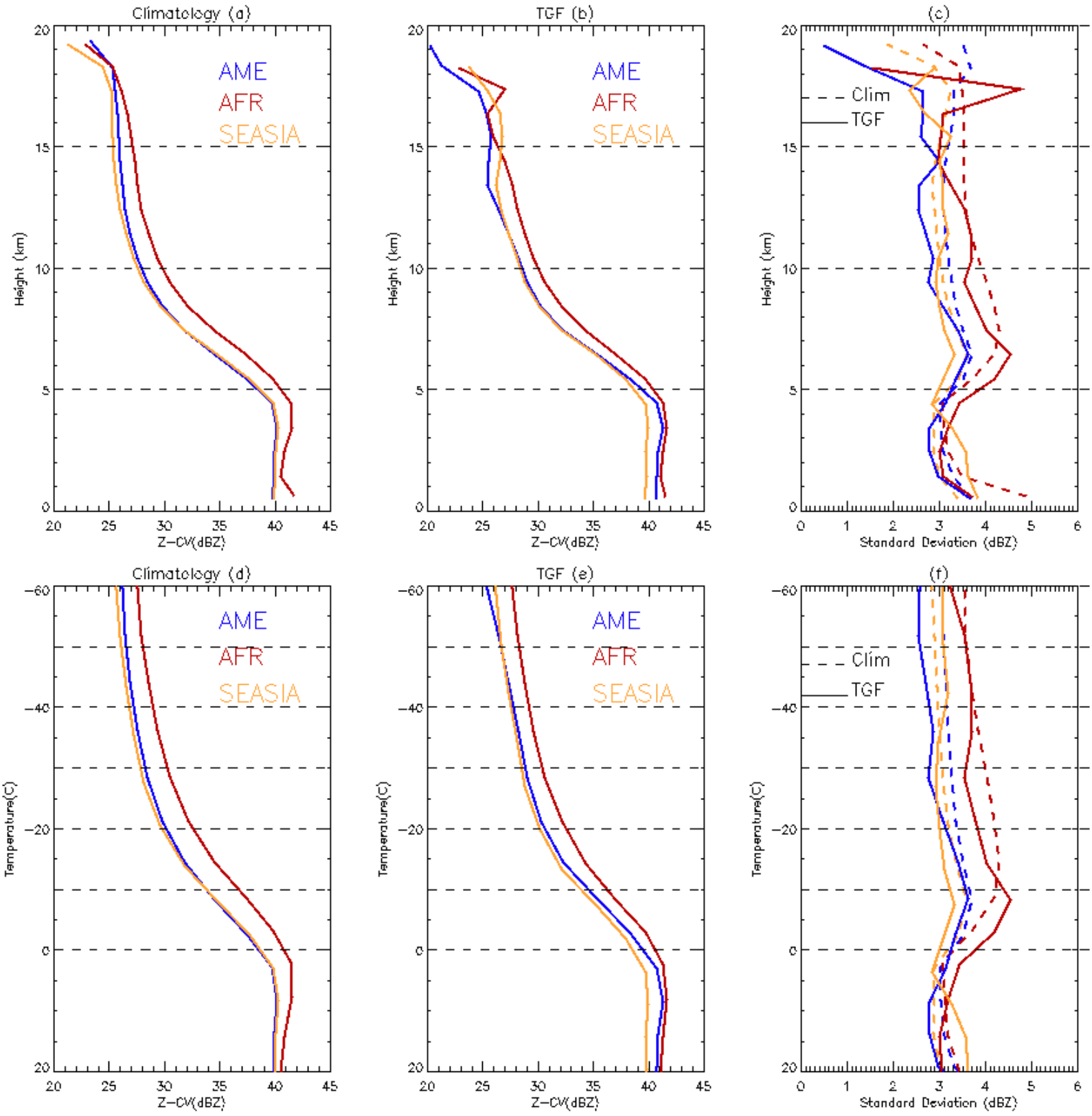
Climatology (a)
TGF (b)
(c)
AME
AFR
SEASIA
Clim
TGF
Height (km)
Z–CV(dBZ)
Standard Deviation (dBZ)
Climatology (d)
TGF (e)
(f)
Temperature(C)

Figure 2.

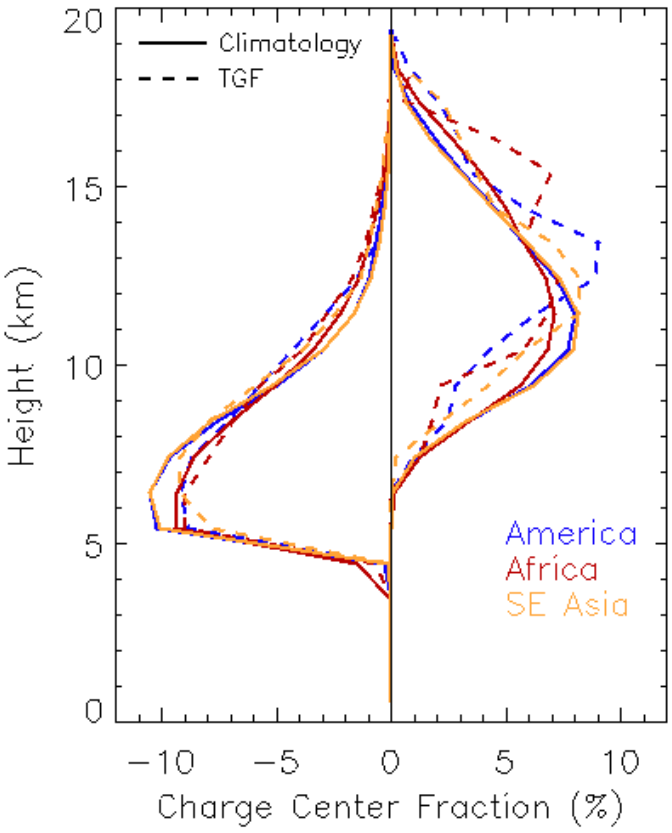
Climatology
TGF
America
Africa
SE Asia
Height (km)
Charge Center Fraction (%)
0
5
10
15
20
−10
−5
0
5
10

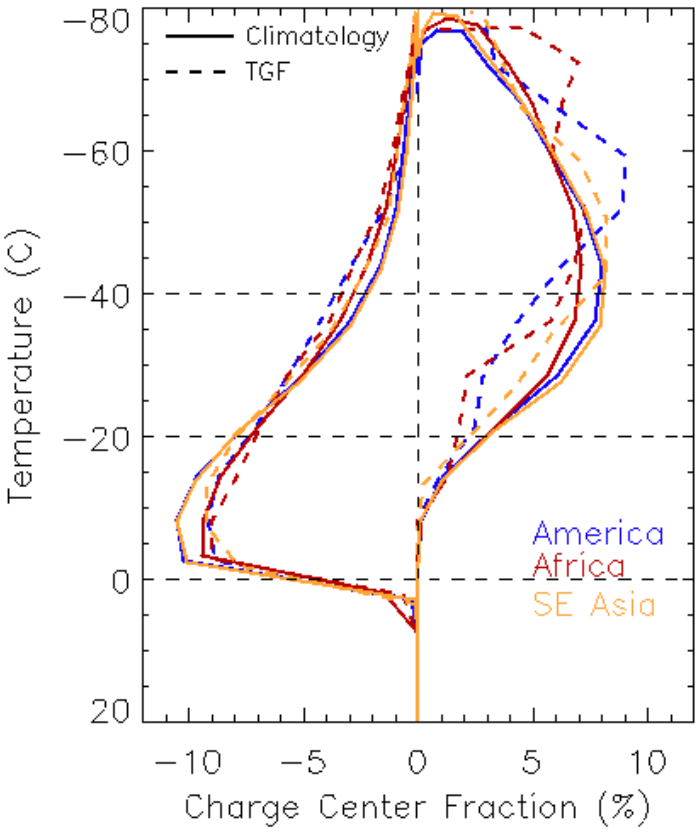
Climatology
TGF
America
Africa
SE Asia
Temperature (C)
Charge Center Fraction (%)
−80
−60
−40
−20
0
20
−10
−5
0
5
10

Tropical TGF Paradox: A Perspective From TRMM Precipitation Radar

Carlos A. Morales Rodriguez[1], Joan Montanyà[2], Ferran Fabró[3], Jesus A. Lopez[2], Oscar A. van der Velde[2]

[1]Departamento de Ciências Atmosféricas, Instituto de Astronomia, Geofísica e Ciências Atmosféricas, Universidade de São Paulo, São Paulo, Brazil

[2]Polytechnic University of Catalonia, Terrassa, Spain

[3]Meteorological Service of Catalonia, Barcelona, Spain

Corresponding Author: carlos.morales@iag.usp.br

Key Points:

- TGF thunderstorms present similar precipitation vertical structure independent of the region;
- The distance between the electrical charging layers dictates the production of TGFs by thunderstorms;
- Southeast Asian and American thunderstorms are more likely to produce TGFs than African counterparts;

2nd Submission: 27 April 2020

Abstract

The Terrestrial Gamma-ray Flashes (TGF) to lightning ratio, computed over the 3 tropical chimneys, presents a paradox: African thunderstorms produce the most lightning but yield the lowest fraction of TGF when compared to American and Southeast Asian thunderclouds. To understand the physical insights into this asymmetry, TRMM Precipitation Radar measurements are used to depict the vertical precipitation structure of the observed thunderstorms in the 3 regions and the thunderstorms during TGF occurrences detected by AGILE, Fermi-GBM and RHESSI sensors. African thunderstorms are taller, smaller and have higher concentration of dense ice particles above the freezing level. TGF thunderstorms are taller and less intense (0.5-2dBZ), besides presenting similar radar reflectivity decay with height independent of the region. In addition, these storms show thicker electrical charge layers separated by 4.7-5.2 km and also a positive charge fraction reduction between -20^{o}C and -40^{o}C and enhancement above -50^{o}C when compared to the overall thunderstorms.

Plain Language Summary

Terrestrial Gamma-ray Flashes (TGF) have been detected above thunderstorms worldwide but its main triggering mechanism has not been fully understood so far. In the last two decades, several measurements from ground and satellite instruments provided information to help our understanding. For instance, TGF emissions are concentrated in the tropics and are believed to be related to intense intra-cloud lightning processes produced by thunderstorms that have well vertically separated charge centers. Although African thunderstorms have the highest lightning activity in the world, they produce less TGFs per lightning than thunderstorms in America and the Southeast Asia tropical regions, posing a paradox. To explore this asymmetry, this study employed 3D measurements from the Precipitation Radar on board the Tropical Rainfall Measuring Mission (TRMM) satellite to describe the main precipitation vertical structure observed in the 3 tropical chimneys and in the thunderstorms that produced TGFs. As a result, African thunderstorms have more lightning discharges because they have more ice aloft and are taller and smaller. The TGF-producing thunderstorms, however, show similar radar reflectivity decay with height independent of the region, in addition to being taller and slightly less intense. Moreover, those thunderstorms present thicker positive electrical charge layers at higher altitudes, which helps to produce stronger intra-cloud lightning.

1 Introduction

Almost 20 years since the discovery of Terrestrial Gamma-ray Flashes (TGF) by *Fishman et al.* (1994), the environment of the source of these sub-millisecond pulse-like emissions of MeV energetic gamma ray photons (*Briggs et al.,* 2010; *Marisaldi et al.,* 2019 and *Østgaard et al.*, 2019) is still not well understood. It is accepted that these emissions are related to intra-cloud lightning processes (e.g. *Cummer et al.,* 2005) but the identification of those thunderstorms that lead to the production of TGFs is a subject of great interest (e.g. *Fabró et al.*, 2019). In the last decade, several space-based missions (e.g. Burst and Transient Source Experiment – BATSE [*Fishman et al.*, 1994, Reuven Ramaty High Energy Solar Spectroscopic Imager - RHESSI [*Smith et al.* 2005], Astrorivelatore Gamma a Immagini Leggero - AGILE [*Marisaldi et al.*, 2010], Fermi Gamma-ray Burst Monitor - Fermi-GBM [*Briggs et al.,* 2010] and Atmosphere-Space Interactions Monitor – ASIM [*Østgaard et al*., 2019]) have observed TGFs worldwide and revealed an asymmetric behavior between the 3 tropical chimneys. Namely, the most prolific lightning producer, the African continent, produces less TGFs per flash rate than the American and Southeast Asian regions (*Smith et al.* 2010, *Splitt et al. 2011*, *Fuschino et al.* 2011, *Briggs et al.* 2013, *Fabro et al.* 2019). Basically, this last study proposed that the higher intra-cloud (IC) rates observed in the African thunderstorms may explain this paradox because those thunderstorms seems to present shorter distances between the electrical charge centers in addition to having higher altitude charge layers when compared to American and Southeast Asian thunderstorms. Consequently, African thunderstorm pose convenient conditions for high IC flash rates, which result in IC discharges with shorter horizontal/vertical extension, less energy and short time duration in contrast to the more energetic lightning flashes observed with TGF (*Cummer et al.,* 2015).

To evaluate the relationship between thunderstorms in the tropical chimney regions and TGF production, the following questions are asked: Does the vertical structure of thunderstorms reproduce the lightning flash rate asymmetry observed in the 3 chimneys?; Is there any signature that explains why African thunderstorms have more IC than CG compared to the American and Southeast Asian thunderstorms?; Are TGF-producing thunderstorms alike independent of the region? Does the vertical distance between the electrical charge centers dictate the production of TGF?

2 Methodology and Data

To understand and explore the microphysical properties observed in this TGF paradox and seek for physical explanations, this study employs worldwide measurements from the Precipitation Radar (PR) (*Yguchi et al.,* 2000) and Lightning Imaging Sensor (LIS) (*Christian et al.,* 1999) on board of the Tropical Rainfall Measuring Mission (TRMM) satellite (*Kummerow et al.,* 1998) observed between 1998 and 2014. For this study, thunderstorms are defined as contiguous rain area with more than 2 TRMM PR pixels with at least one LIS lightning flash within the field of view (*Morales Rodriguez*, 2019). To diagnose the thunderstorms observed in the tropical chimneys, we analyze the mean 3D precipitation structure observed in the 3 thunderstorms regions (America, African and SE Asia) with maximum TGF activity as shown in *Fabró et al.* (2019) (Table 1) in an area of 20 x 20 degrees.

To test if the 3D precipitation features can explain the TGF paradox, we analyze the TGF related TRMM thunderstorms, i.e., thunderstorms that were observed near TGF detections from AGILE (*Marisaldi et al.*, 2010) (2009-03-02 to 2012-07-30), Fermi-GBM (*Briggs et al.,* 2010) (2008-08-07 to 2014-12-31), and RHESSI (*Smith et al.* 2005) (2002-03-04 to 2010-09-06). As these missions could not detect the precise TGF location and simultaneous TRMM overpasses are unlikely, we propose to seek the nearest active thunderstorm, similar to *Barnes et al.* (2015) that used TRMM Microwave Imager (TMI) overpasses within ± 1 hour and 500 km from RHESSI TGF reported locations to characterize the microphysical properties of TGF and non-TGF storms. For our procedure, we select the closest thunderstorm observed by TRMM-PR within +/- 30 minutes of the TGF detection and up to 600 km from the TGF triggered location (AGILE, Fermi-GBM and RHESSI) provide. By doing this, we are assuming that these thunderstorms may capture the closest microphysical characteristics observed during the lifecycle of TGF related clouds. The number of analyzed TRMM orbits in the three regions and the number of thunderstorms extracted from those orbits are summarized in Table 1. Additionally, Table 1 presents the number of TRMM-PR orbits with coincident TGF observations from AGILE, Fermi-GBM and RHESSI satellite missions that met the distance and time criteria defined before. Furthermore, only TRMM-PR convective rain type profiles (*Awaka et al*., 1997) are used for this analysis. NOAA National Center for Environmental Prediction (NCEP) and National Center of Atmospheric Research (NCAR) reanalysis (Reanalysis-1) (*Kalnay et al.*, 1996) were later used to convert TRMM PR heights into temperature by using the vertical temperature and geopotential height observed in the location and date of TRMM overpass using the same procedure shown by *Morales Rodriguez* (2019).

To verify the predominance of intra-cloud activity or not in the three aforementioned regions, we computed the intra-cloud (IC) to cloud-to-ground (CG) ratio based on *Boccippio et al.* (2001). LIS 0.1x0.1 degree flash rate climatology (*Albrecht et al.,* 2016) has been used as total lightning activity while WWLLN flash density from the period of 2012-2018 has been used for CG. For this method, LIS detection efficiency (DE) was configured as 0.8 for IC and 0.4 for CG (*Boccippio et al*., 2001), while WWLLN which measures essentially CG was initially normalized to its hourly/daily relative DE (*Hutchins et al*., 2012) and then converted to flashes by applying a stroke multiplicity of 1.5 (Burgesseur, 2017) and finally corrected with a CG DE of 0.1 (mean value from Rodgers et al., 2006; Abarca et all., 2011; Rudlosky et al., 2013).

Finally, to test the statistical representativeness of the difference between the thunderstorms databases, we computed the Student's *t* test for the difference of means of two distributions (Wilks, 2011). The *p-level* obtained by the Z score will provide the statistical significance of the difference of the means.

Table 1. Number of TRMM orbits and the respective number of thunderstorms observed in each tropical chimney during the period of 1998 and 2014 and the number of TRMM orbits associated with TGFs detected by AGILE, Fermi-GBM and RHESSI satellite missions during their period of observation.

	TRMM		
Region	Orbits	Thunderstorms	Number of Orbits with coincident TGF
America (90-70W & 0-20N)	3,690	11,391	35
Africa (15-35E & 10S-10N)	4,089	23,656	43
Southeast Asia (95-115E & 10S-10N)	1,993	6,117	45

3 Results

From Table 1 it is possible to observe that African continent presents the highest frequency of occurrence of thunderstorms followed by America and Southeast Asia region, consistent with the climatologies presented by *Boccippio et al.* (2000), *Cecil et al*. (2014) and *Albrecht et al.* (2016). In respect to size and lightning rates observed during TRMM-PR and LIS overpasses, African thunderstorms are smaller (15-20%) but produce much more lightning (1.3-1.9 times more) than the other two areas (see Table 2 and Supplementary Figure S1). American and Southeast Asian thunderstorms are pretty much alike on size and lightning flash rates, although all 3 regions have different means at a confidence level of 99.9%.

In terms of precipitation vertical structure, the vertical profiles of radar reflectivity factor (Z) in Figure 1a and Table 3 show that African thunderstorms are indeed taller and more vigorous than American and Southeast Asian thunderstorms. For instance, African thunderstorms are up to 1.5-2.8 dBZ more intense between 5-15 km height, in addition to Z diminishing faster with altitude than in the other thunderstorms (confidence level of 99.9%). Moreover, African thunderstorms show as much as 1.2 km higher 30 dBZ echo top height than the American and Southeast Asian thunderclouds. These results reinforce indeed that African thunderstorms present stronger updrafts, thus producing more ice efficiently (*Liu et al*., 2012). In fact, intense vertical velocity helps to produce higher super-saturation which activates more cloud condensation nuclei and therefore produces more super-cooled water droplets and ice particles (*Korolev*, 2007). Additionally, Z decreases around 1.5 and 3 dBZ/km between 5 and 8 km height (0 and -25^{o}C) in all three regions, Figure 1a, indicating that riming and accretion is active and very effective. Therefore, the charge electrification processes becomes more efficient (*Takahashi*, 1978; *Saunders et al.*, 2006).

Table 2. Median values (25-75% percentiles in brackets) for thunderstorm radius, number of flashes per thunderstorm, flash density and IC:CG ratio over the 3 regions. LIS flashes correspond to maximum of 90 seconds of TRMM-LIS view time observation (*Christian et al., 1999*).

Region	Radius (km)	LIS Flashes/ thunderstorm	10^3 x LIS Flashes/ thunderstorm.km^2	IC:CG
America	29.0 [17.8-52.0]	3 [1-7]	1.2[0.5-3.0]	0.43 [0.18-0.86]
Africa	22.0 [14.1-38.9]	4 [2-13]	3.0[1.3-6.7]	5.30 [3.72-7.43]
Southeast Asia	27.5 [17.6-47.2]	3 [1-7]	1.3[0.5-3.0]	0.49 [0.21-0.99]

In terms of temperature, Figure 1d, it is possible to confirm that African thunderstorms present the highest Z values in the mixed zone (0 and -40°C) in the convective area (confidence level of 99.9%). Moreover, the 30 dBZ echo height in Africa is found at levels 8-9°C colder than America and Southeast Asia, Table 3. These results indicate that African thunderstorms might have more super-cooled water droplets and denser ice particles aloft in the entire column resulting in a thicker ice layer. Below the 0°C isotherm, Z decreases slightly for African thunderstorms, which may imply that evaporation dominates the collision and breakup processes (*Liu and Zipser*, 2013), while in Southeast Asia and America it is balanced. According to *Fabrò et al.* (2019), African region is drier than the other two areas, consistent with the presented Z profiles.

Table 3. Statistical parameters (mean and p-values from Student *T* test) for the 30 dBZ echo top height (temperature) for coincident measurements of TRMM-PR and LIS over the 3 chimneys (Climatology) and for the thunderstorms associated with AGILE, Fermi-GBM and RHESSI TGF detections. The statistical test evaluates if the Climatology and TGF echo top height (temperature) mean differences are significant.

Region	Climatology	TGF Thunderstorms	*p-values*
America	8.1 km (-19.8°C)	8.7 km (-24.2°C)	0.0516(0.0559)
Africa	9.2 km (-27.7°C)	9.1 km (-26.9°C)	0.4225(0.4052)
Southeast Asia	8.0 km (-18.8°C)	8.7 km (-22.4°C)	0.0228(0.0475)

The radar reflectivity difference in the mixed zone and the echo top height/temperature found among the thunderstorms clearly supports why African thunderstorms present higher lightning activity. By using the inferred IC:CG ratio from LIS and WWLLN lightning flash density around the globe, Table 2 shows that African thunderstorms produce as much as 10-12 more IC discharges per CG flashes than American and Southeast Asian thunderstorms. This can be a response to the higher and thicker ice layer aloft in the African thunderstorms that can help to produce more lightning discharges at higher level. Consequently, this behavior would help to produce shorter and less energetic lightning flashes that in principle would not trigger TGFs, since it is associated with energetic upward leaders. (*Cummer et al.*, 2015).

Until this point, it has been possible to explain physically why African thunderstorms are more prolific lightning producer and have a higher IC:CG ratio than the other 2 chimneys. To further understand why those thunderstorms do not produce as high TGF per flash rate as the American and Southeast Asian thunderstorms, we will discuss the vertical precipitation structure for the thunderstorms that might be related or associated with the occurrence of TGFs during their lifecycle. To do that, we use the TGF databases produced by AGILE, Fermi-GBM and RHESSI satellite missions and identify the correspondent TRMM PR overpasses and select the closest TRMM thunderstorms in distance (just one thunderstorm for each coincident TRMM PR orbit) as explained in the methodology. Based on this procedure, it was possible to identify 35 TGF related thunderstorms in America, 43 in Africa and 45 in Southeast Asia, Table

1. Note that Africa has the lowest ratio between the number of observed thunderstorms by TRMM versus the number of thunderstorms with detected TGF.

Figures 1b and 1e show the mean vertical profile of radar reflectivity as a function of height and temperature respectively, for convective rain type, observed for thunderstorms associated with TGFs in Africa, America and Southeast Asia. The TGF vertical profiles are analogous in shape, Z decreases around 2.5 – 3 dBZ from 0^{o}C to -20^{o}C and between 0.5-1.5 dBZ along the isotherms of -20^{o}C and -40^{o}C. Nonetheless, African thunderstorms have higher reflectivity values than the other two regions (at confidence level of 99%: 4-17 km for America and 2-17 km for SE-Asia). By comparing the Climatology and TGF thunderstorms vertical profiles between the same regions, Figure 1a and 1b, it is found that TGF associate with lower radar reflectivity values. For instance, African TGF thunderstorms are in the order of 1-2 dBZ lower, while a decrease of 0.5-1.3 dBZ is observed in America above 12 km and over 9 km in SE-Asia (Student's *t* test at the confidence level of 99%). In terms of 30 dBZ echo top height and temperature, Table 3, it is observed that American and SE-Asian TGF thunderstorms deepen 600 m and reach as much as 3.5-4.3^{o}C cooler levels (confidence level above 94%), while less significant African thunderstorms that shrink 100 meters. Despite the mean values difference, TGF thunderstorms are alike in radar reflectivity changes with height and temperature independently of the region. Secondly, to produce TGF, African thunderstorms need to resemble American and Southeast Asian.

To further explore how those 3D precipitation features are related to electric charge layers, we employed the Takahashi (1978) study that retrieved experimentally the charge transferred during the collisions between graupel formed by super-cooled water droplets and ice particles. Basically, for each mean vertical profile extracted, we computed the polarity gained by the ice particles by means of the liquid water content and temperature at each level. To convert radar reflectivity to liquid water content, we employed the relationship of *Oh et al.* (2018). Then, for each vertical profile we have a profile of positive and negative charges gained, and then we normalized to obtain the same amount of positive and negative charges for every profile to guarantee that the net charge is zero.

Figure 2 compares the mean electric charge polarity profile estimated for the 3 chimneys areas and for the cases with TGFs respectively. The estimated profiles show 2 main charge centers (10-90% percentile): a) midlevel negative charge center varying from 4.8 to 10.8 (0 to -38.9^{o}C); b) positive charge center located at upper levels, i.e., from 8.5 to 15.6 km (-21.4 to -73.2 ^{o}C). When comparing the charging fractions, a Student´s *T* test shows a statistically significant difference amongst the profiles: a) Positive charges (95% level of confidence) – America shows a difference between 6-15 km, Africa from 8-11 and 14-16 km and SE-Asia from 6-11 and 12-14 km; b) Negative charges (99.9% level of confidence) – America presents differences between 5-13 km, Africa from 4-6 and 9-13 km and SE-Asia from 4-13 km. Furthermore, TGF thunderstorms show a vertical displacement of the charge centers (median charge height layer as a reference). The upper positive charge layer moves upward by 800 to 1200 m (5.2 to 9.1 ^{o}C colder). The negative charge center shifts aloft 300 to 400 m (1.5 to 2.2 ^{o}C colder). The distance between the negative and positive charge centers varies from 4.3-4.6 km for overall thunderstorms to 4.7-5.2 km for TGF-associated thunderstorms, reinforcing that thunderstorms that produce TGF are expected to show more vertically separated charging

centers, which are associated with more energetic lightning flashes (*Fabró et al.,* 2019). Additionally, TGF thunderstorms show slightly thicker (300-600 m) positive and negative charge layers. Lastly, African TGF thunderstorms present regions of positive charges that extend up to 15.5 km, Figure 2a. All these features reinforce the higher IC flash rates observed in African thunderstorms and the lower TGF efficiency. Using the radar reflectivity profile of Figure 1e, it can be speculated that the decrease of the charge density between -20 ^{o}C and -40^{o}C observed in the TGF thunderstorms (Figure 2b) is caused by a decrease in the hail production, which reduces the size of these dense particles. The charge fraction enhancement at temperatures below -50^{o}C might be an effect of more ice particles produced by sublimation and aggregation processes that collide with the smaller graupel/hail particles formed in the mixed zone.

4 Conclusions

We presented a statistical study that analyzed the vertical structure of thunderstorms observed in 9,772 TRMM PR orbits to elucidate the TGF versus lightning occurrence asymmetry observed between the 3 major tropical thunderstorm regions. Mean profiles were computed using TRMM PR and LIS coincident measurements from 1998 to 2014. TGFs detected by AGILE, Fermi-GBM and RHESSI instruments were used as proxies to select the most probable associated precipitation feature in the field of view of these sensors.

According to the vertical precipitation structures in convection over America, Africa and Southeast Asia regions, African thunderstorms present higher concentration of super-cooled water droplets and ice particles above the freezing level as these thunderstorms show higher Z values (1.5-2.8 dBZ) above the 0^{o}C isotherm. African thunderstorms are smaller (5-20%), 1.2 km taller and 9^{o}C colder (30 dBZ echo top height). Furthermore, taking into account LIS measurements, African thunderstorms produce almost 30-80% more lightning flashes than their American and Southeast Asian counterpart thunderclouds. Moreover, by using the IC:CG ratio retrieved with LIS and WWLLN data, Africa shows as much as 10-12 times more IC lightning than the other two regions.

TGF related thunderstorms present similar radar reflectivity decay with height and temperature independently of the region. In general TGF thunderstorms are less intense (by 0.5-2 dBZ) and taller in respect to the climatology. Among the TGF thunderstorms profiles, Africa tends to resemble the other two regions in vertical shape despite being more intense in terms of radar reflectivity (1-2 dBZ).

After estimating the electric charge layer altitudes by employing *Takahashi's* (1978) scheme, it was possible to find that a cloud microphysical mechanism contributes to the production of TGFs. Basically the cloud water content profile changes the height and distance between the positive and negative charge centers. TGF thunderstorms have thicker charging layers separated by a distance of 4.7-5.2 km while the climatology set of storms shows a distance between 4.3-4.6 km. Additionally, TGF thunderstorms presented a vertical expansion of 600 meters of the positive charge layer. In terms of temperature, the positive charge fraction decreases between -20^{o}C and -40^{o}C and increases above -50^{o}C observed in the TGF thunderstorms may be related to the production of small graupel and hail particles in the mixed region that are lifted to upper levels and collide with the small ice particles formed by

either water vapor deposition or aggregation. These changes are consistent with *Barnes et al.* (2015) work that showed that TGF related thunderstorms have higher cloud and precipitating ice and cloud ice concentration above 9 km in comparison with non TGF thunderstorms. Lastly, African TGF thunderstorms present an upper positive charge peak extending from 12 to 15.5 km, which may indicate the existence of a competition among the opposite charge centers that creates shorter IC channels, thus carrying less charges. Therefore, by increasing the distance of the charge layers, lightning discharges become less frequent, which helps to build the electric field without competition, thus producing more energetic discharges due to the larger path to breakdown.

In conclusion, it has been possible to identify with this methodology that the distance between the opposite electrical charge centers and its relative altitude position control the production of stronger and weaker IC discharges that might be connected with TGF production or not, respectively.

Acknowledgements

This work was supported by the following research grants: Brazilian Research Agencies - Conselho Nacional de Desenvolvimento Científico e Tecnológico (CNPq) [grant numbers: 310489/2006-7] and Coordenação de Aperfeiçoamento de Pessoal de Nível Superior (CAPES) – Programs PROEX and PrInt (grant number: 88887.370081/2019-00); Spanish Ministry of Economy and the European Regional Development Fund (FEDER): ESP2013-48032-C5-3-R, ESP2015-69909-C5-5-R and ESP2017-86263-C4-2-R. The authors are grateful to TRMM Science Data and Information System (TSDIS) of Goddard Space Flight Center for providing TRMM/PR orbits, to the Lightning and Atmospheric Electricity Group at NASA's Marshall Space Flight Center for their support of the TRMM/LIS data files, to National Centers for Environmental Information (NOAA) for providing NCEP/NCAR Reanalysis (Reanalysis-1), to the Italian Space Agency for providing AGILE TGF data, to David Smith at the University of California, Santa Cruz, for making available RHESSI TGF collection and to NASA Fermi-GBM´s Mission for Fermi-GBM TGF database. The authors wish to thank the World Wide Lightning Location Network (http://wwlln.net), collaboration among over 50 universities and institutions, for providing the lightning location data used in this paper. All of the data used in this manuscript are publicly available on the STORM-T Laboratory website data repository (at http://www.storm-t.iag.usp.br/pub/TGF-Paradox).

References

Abarca, S. F., Corbosiero, K. L., & Galarneau Jr, T. J. (2010). An evaluation of the worldwide lightning location network (WWLLN) using the national lightning detection network (NLDN) as ground truth. *Journal of Geophysical Research: Atmospheres*, *115*(D18).

Albrecht, R. I., Goodman, S. J., Buechler, D. E., Blakeslee, R. J., & Christian, H. J. (2016). Where are the lightning hotspots on Earth?. *Bulletin of the American Meteorological Society*, *97*(11), 2051-2068.

Awaka, J., T. Iguchi, H. Kumagai, and K. Okamoto, 1997: Rain type classification algorithm for TRMM precipitation radar. *Proc. 1997 Int. Geoscience and Remote Sensing Symp.,* Singapore, IEEE, 1633–1635.

Barnes, DE, Splitt, ME, Dwyer, JR, Lazarus, S, Smith, DM, and Rassoul, HK (2015), A study of thunderstorm microphysical properties and lightning flash counts associated with terrestrial gamma-ray flashes. *J. Geophys. Res. Atmos.*, 120, 3453– 3464. doi: 10.1002/2014JD021495.

Boccippio, D. J., Goodman, S. J., & Heckman, S. (2000). Regional differences in tropical lightning distributions. *Journal of Applied Meteorology*, *39*(12), 2231-2248.

Briggs, M. S., et al. (2010), First results on terrestrial gamma ray flashes from the Fermi Gamma-ray Burst Monitor, J. Geophys. Res., 115, A07323, doi:10.1029/2009JA015242.

Bürgesser, R. E. (2017). Assessment of the world wide lightning location network (WWLLN) detection efficiency by comparison to the lightning imaging sensor (LIS). *Quarterly Journal of the Royal Meteorological Society*, *143*(708), 2809-2817.

Cecil, D. J., Buechler, D. E., & Blakeslee, R. J. (2014). Gridded lightning climatology from TRMM-LIS and OTD: Dataset description. *Atmospheric Research*, *135*, 404-414.

Christian H, Blakeslee R, Goodman S, Mach D, Stewart M, Buechler D, Koshak W, Hall J, Boeck W, Driscoll K, Bocippio DJ. The lightning imaging sensor.*In NASA conference publication* 1999 Jun 7 (pp. 746-749).NASA.

Cummer, S. A., Zhai, Y., Hu, W., Smith, D. M., Lopez, L. I., & Stanley, M. A. (2005). Measurements and implications of the relationship between lightning and terrestrial gamma ray flashes. *Geophysical Research Letters*, 32, L08811. https://doi.org/10.1029/2005GL022778.

Cummer, S.A., Lyu, F., Briggs, M.S., Fitzpatrick, G., Roberts, O.J. and Dwyer, J.R., 2015. Lightning leader altitude progression in terrestrial gamma-ray flashes. *Geophysical Research Letters*, *42*(18), pp.7792-7798.

Dowden, R. L., J. B. Brundell, and C. J. Rodger (2002), VLF lightning location by time of group arrival (TOGA) at multiple sites, *J. Atmos. Sol. Terr. Phys.*, **64**, 817–830

Fabró Tàpia, F., Montañá Puig, J., der Velde, V., Arnoud, O., Pineda Rüegg, N., & Williams, E. R. (2019). On the TGF/lightning ratio asymmetry. *Journal of geophysical research: atmospheres*, 1-31.

Fishman, G. J., Bhat, P. N., Mallozzi, R., Horack, J. M., Koshut, T., Kouveliotou, C., ... & Goodman, S. J. (1994). Discovery of intense gamma-ray flashes of atmospheric origin. *Science*, *264*(5163), 1313-1316.

Gjesteland, T., N. Østgaard, a. B. Collier, B. E. Carlson, C. Eyles, and D. M. Smith (2012), A new method reveals more TGFs in the RHESSI data, Geophysical Research Letters, 39 (5), doi:10.1029/2012GL050899.

Iguchi T, Kozu T, Meneghini R, Awaka J, Okamoto KI. Rain-profiling algorithm for the TRMM precipitation radar.*Journal of Applied Meteorology*. 2000 Dec;39(12):2038-52.

Joss, J. and Pittini, A.: Real-time estimation of the vertical profile of radar reflectivity to improve the measurement of precipitation in an Alpine region, Meteorol. Atmos. Phys, 47, 61–72, https://doi.org/10.1007/BF01025828, 1991.

Kalnay, E., Kanamitsu, M., Kistler, R., Collins, W., Deaven, D., Gandin, L., ... & Zhu, Y. (1996). The NCEP/NCAR 40-year reanalysis project. *Bulletin of the American meteorological Society*, *77*(3), 437-472

Korolev, A. (2007). Limitations of the Wegener–Bergeron–Findeisen mechanism in the evolution of mixed-phase clouds. *Journal of the Atmospheric Sciences*, *64*(9), 3372-3375.

Kummerow, C., Barnes, W., Kozu, T., Shiue, J., & Simpson, J. (1998).The tropical rainfall measuring mission (TRMM) sensor package. *Journal of atmospheric and oceanic technology*, *15*(3), 809-817.

Liu, C., Cecil, D. J., Zipser, E. J., Kronfeld, K., and Robertson, R. (2012), Relationships between lightning flash rates and radar reflectivity vertical structures in thunderstorms over the tropics and subtropics, *J. Geophys. Res.*, 117, D06212, doi:10.1029/2011JD017123.

Liu, C., & Zipser, E. J. (2013). Why does radar reflectivity tend to increase downward toward the ocean surface, but decrease downward toward the land surface? *Journal of Geophysical Research: Atmospheres*, *118*, 135–148. https://doi.org/10.1029/2012JD018134

Marisaldi, M., et al. (2010a), Detection of terrestrial gamma ray flashes up to 40 MeV by the AGILE satellite, J. Geophys. Res., 115, A00E13, doi:10.1029/2009JA014502.

Marisaldi, M., Galli,M., Labanti, C., Ostgaard, N., Sarria, D., Cummer, S. A., et al. (2019). On the high-energy spectral component and fine time structure of terrestrial gamma-ray flashes. *Journal of Geophysical Research: Atmospheres*, 124, 7484–7497. https://doi.org/10.1029/2019JD030554

Morales Rodriguez, C. A. (2019). Thunderstorm efficiency regimes in South America as observed by STARNET and TRMM. *Journal of Geophysical Research: Atmospheres*, 124, 11428–11451. https://doi.org/10.1029/2019JD030950

Oh, S-B, Kollias, P, Lee, J-S, Lee, S-W, Lee, YH, Jeong, J-H. Rain-rate estimation algorithm using signal attenuation of Ka-band cloud radar. *Meteorol Appl*. 2019; 1–13. https://doi.org/10.1002/met.1825.

Østgaard, N., Neubert, T., Reglero,V., Ullaland, K., Yang, S., Genov, G.,et al. (2019). First 10 months of TGF observations by ASIM. *Journal of Geophysical Research: Atmospheres*,124. https://doi.org/10.1029/2019JD031214

Rodger, C. J., Werner, S., Brundell, J. B., Lay, E. H., Thomson, N. R., Holzworth, R. H., & Dowden, R. L. (2006). Detection efficiency of the VLF World-Wide Lightning Location Network (WWLLN): initial case study.

Rudlosky, S. D., & Shea, D. T. (2013). Evaluating WWLLN performance relative to TRMM/LIS. *Geophysical Research Letters*, *40*(10), 2344-2348.

Saunders, C. P. R., Bax-Norman, H., Emersic, C., Avila, E. E., & Castellano, N. E. (2006). Laboratory studies of the effect of cloud conditions on graupel/crystal charge transfer in thunderstorm electrification. *Quarterly Journal of the Royal Meteorological Society: A journal of the atmospheric sciences, applied meteorology and physical oceanography*, *132*(621), 2653-2673.

Smith, D. M., et al. (2005), Terrestrial gamma-ray flashes observed up to 20 MeV, Science, 307, 1085–1088.

Splitt ME, Lazarus SM, Barnes D, Dwyer JR, Rassoul HK, Smith DM, Hazelton B, Grefenstette B. (2010), Thunderstorm characteristics associated with RHESSI identified terrestrial gamma ray flashes. *Journal of Geophysical Research: Space Physics*. 2010 Jun 1;115(A6).

Takahashi, T. (1978). Riming electrification as a charge generation mechanism in thunderstorms. *Journal of the Atmospheric Sciences*, *35*(8), 1536-1548.

Figure 1. Mean vertical radar reflectivity and respective standard deviations profiles for convective rain type as a function of height (top) and temperature (lower) in the 3 chimneys: America (blue), Africa (red) and Southeast Asia (orange). (a) and (d) plots are for climatology profiles and (b) and (e) for TGF detections from AGILE, Fermi-GBM and RHESSI. (c) and (f) show the standard deviation for climatology (dashed) and TGF (continuous) profiles as function of altitude and temperature respectively.

Figure 2. Mean vertical profile of charge fraction estimated for all 3 chimneys (Climatology - continuous) and TGF triggered thunderstorms (dashed) based on *Takahashi* (1978) scheme as a function of height (a) and temperature (b). The negative and positive charge centers have each a total of 50% of the total charges.